



Open Research Online

The Open University's repository of research publications and other research outputs

Lithium abundances from the 6104 Å line in cool Pleiades stars

Journal Item

How to cite:

Ford, A.; Jeffries, R. D. and Smalley, B. (2002). Lithium abundances from the 6104 Å line in cool Pleiades stars. *Astronomy & Astrophysics*, 391(1) pp. 253–265.

For guidance on citations see [FAQs](#).

© 2002 ESO

Version: Version of Record

Link(s) to article on publisher's website:

<http://dx.doi.org/doi:10.1051/0004-6361:20020779>

Copyright and Moral Rights for the articles on this site are retained by the individual authors and/or other copyright owners. For more information on Open Research Online's data [policy](#) on reuse of materials please consult the policies page.

oro.open.ac.uk

Lithium abundances from the 6104 Å line in cool Pleiades stars

A. Ford^{1,2}, R. D. Jeffries¹, and B. Smalley¹

¹ Department of Physics, Keele University, Keele, Staffordshire, ST5 5BG, UK

² Department of Physics and Astronomy, The Open University, Walton Hall, Milton Keynes, MK7 6AA, UK
e-mail: alison.ford@open.ac.uk; rdj@astro.keele.ac.uk or bs@astro.keele.ac.uk

Received 7 January 2002 / Accepted 17 May 2002

Abstract. Lithium abundances determined by spectral synthesis from both the 6708 Å resonance line and the 6104 Å subordinate line are reported for 11 Pleiades late-G and early-K stars observed at the William Herschel Telescope. Firm detections of the weak subordinate line are found for four objects, marginal detections for four, and upper limits for the remaining three stars. Some of these spectra were previously analysed by Russell (1996), where he reported that abundances derived from the 6104 Å line were systematically higher than those obtained from the 6708 Å line by 0.2–0.7 dex. He also reported a reduced spread in the 6104 Å line abundances compared with those determined from the 6708 Å feature. Using spectral synthesis we have re-analysed Russell’s data, along with our own. Our results do not entirely support Russell’s conclusions. We report a ~0.7 dex scatter in the abundances from 6708 Å and a scatter at least as large from the 6104 Å line. We find that this is partly explained by our inclusion of a nearby Fe II line and careful modelling of damping wings in the strong metal lines close to the 6104 Å feature; neglect of these leads to overestimates of the Li abundance which are most severe in those objects with the weakest 6104 Å lines, thus reducing the abundance scatter. We find a reasonable correlation between the 6104 Å and 6708 Å Li abundances, although four stars have 6104 Å-determined abundances which are significantly larger than the 6708 Å-determined values by up to 0.5 dex, suggesting problems with the homogeneous, 1-dimensional atmospheres being used. We show that these discrepancies can be explained, although probably not uniquely, by the presence of star spots with plausible coverage fractions. The addition of spots does not significantly reduce the apparent scatter in Li abundances, leaving open the possibility that at least some of the spread is caused by real star-to-star differences in pre-main sequence Li depletion.

Key words. stars: abundances – stars: late type – stars: interiors – open clusters and associations: individual: Pleiades

1. Introduction

The observed spread of lithium abundances in stars of the young (~100 Myr) zero-age main sequence (ZAMS) Pleiades cluster has been puzzling observers for around 20 years. The spread appears at $T_{\text{eff}} \sim 5800$ K and continues into cooler stars. The magnitude of the spread increases with decreasing mass and reaches a maximum (more than 1 dex) at $0.8 M_{\odot}$ in the mid-K stars before possibly decreasing in the coolest objects (Jones et al. 1996). Duncan & Jones (1983) first reported the scatter, and interpreted it as being due to a large (~0.4 Gyr) age spread within the cluster stars, although this has since been shown to be unlikely (Soderblom et al. 1993a). A scatter is also seen in other young clusters (e.g. Randich 2001), but diminishes by the age of the Hyades (Soderblom et al. 1995 – although most Li data for Hyades K stars are upper limit estimates). Pasquini et al. (1997) report evidence that the spread

reappears with a dispersion >1 dex among the solar-type stars of the old (~5 Gyr) M 67 cluster.

Soderblom et al. (1993a) noted that there is a connection between rotation and Li abundance in these cool stars, in the sense that rapid rotators seem to display higher Li abundances. Jeffries (2000) showed that *slow* rotators can have *either* high *or* low abundances. In addition, there is a correlation with chromospheric activity, with more-active stars also showing more lithium. It is not clear whether this link is causal or coincidental: i.e. whether star spots or other chromospheric effects give rise to an *apparent* abundance spread (Stuik et al. 1997; King et al. 2000), or if the spread is real and linked to activity through a physical mechanism connected with the rotation in these objects (Soderblom et al. 1993a; Jones et al. 1997). For instance, non-standard effects such as rotation-driven mixing (e.g. Chaboyer et al. 1995) or perhaps even metallicity differences between individual cluster stars could cause variations in star-to-star lithium depletion during the PMS phase.

Almost all Li abundance measurements in main sequence Pop. I and Pop. II stars have been made using the strong

Send offprint requests to: A. Ford,
e-mail: alison.ford@open.ac.uk

Table 1. Observational information for new data obtained for this paper and for data from Russell (1996).

| | This paper | | Russell (1996) |
|----------------------|-----------------------------|-----------------------------|-----------------------------|
| Observation date | 1998 11 28–29 | 1999 12 22–23 | 1993 01 08–10 |
| Echelle grating | E31 | E31 | E31 |
| Detector | SITe1 | SITe1 | EEV6 |
| Pixel size | 24.0 μm | 24.0 μm | 22.5 μm |
| Dispersion at 6104 Å | 0.061 Å pixel ⁻¹ | 0.061 Å pixel ⁻¹ | 0.057 Å pixel ⁻¹ |
| Central wavelength | 5875 Å | 5814 Å | 6770 Å |
| Exposure time | 9000 s (5 × 1800 s) | 6000 s (5 × 1200 s) | 3600 s (3 × 1200 s) |
| Resolving power | 50 000 | 40 000 | 48 000 |

Li I 6708 Å resonance line. This line is formed high in the atmosphere and samples a limited range of depths. It is plausible that it could be affected by chromospheric activity (Houdebeine & Doyle 1995) or other inhomogeneities such as star spots (Giampapa 1984), leading to erroneous Li abundances. Stuijk et al. (1997) argue that the effects of the chromosphere are primarily communicated through photospheric stratification and ionizing radiation fields, and therefore by changes in the ionization balance. To first order, all the alkali lines should be similarly affected by the presence of a chromosphere. Indeed, a number of authors have noted that the K I line at 7699 Å also shows some evidence for a spread in strength at the same effective temperatures, although perhaps not as large as for Li I 6708 Å (Soderblom et al. 1993a; Jeffries 1999; King et al. 2000).

Explaining the observed spread in Li abundances among such a group of co-eval stars is an important goal. Either the abundance spread is real, which would tell us that non-standard mixing processes (those additional to convection) can produce star-to-star differences, probably as a result of differing angular momenta, or that there really is no abundance spread; in which case the observations would tell us that crude, one-component, plane-parallel atmospheres poorly describe conditions in young, convective stars where there might be additional turbulence or atmospheric inhomogeneities to contend with.

A crucial test of the reliability of atmospheres used in Li abundance analyses would be to obtain the abundance using alternative lines. Unfortunately the available optical lines (the subordinate transitions at 6104 Å and 8126 Å) are very weak and blended with other strong metal features. Nevertheless, these lines sample different depths within the atmosphere and the lower levels of their transitions form the upper level for the resonance line. It is, therefore, of primary importance to determine Li abundances from these lines separately, and to compare them with abundances measured from the resonance line.

Russell (1996) measured 6104 (hereafter “6708” and “6104” are taken to mean “the Li I resonance line at 6708 Å” and “the Li I subordinate line at 6104 Å” respectively) in the atmospheres of six Pleiades late-G/early-K stars, and compared the abundances to those measured from 6708. His results suggested that 6104 gave abundances which were systematically higher than those from 6708 by 0.2–0.7 dex. He also reported a significantly smaller Li abundance spread derived from 6104. If Russell’s conclusions were correct, they would indicate that something is seriously wrong with the model atmospheres used in such abundance determinations. The combination of a

reduction in spread from one line over the other, and an abundance discrepancy between the two lines would suggest that there are problems with the temperature structure of the atmospheres, possibly related to inhomogeneities such as spots or plagues on the stellar surface. However, Martín (1997) claims that Russell has probably overestimated the strength of the subordinate line by a factor of 2 or 3, due to his use of an inappropriate Gaussian-fitting technique. If this is taken into account, Martín believes that the abundances from the two lines might agree to within 0.2 dex; in this case the agreement between the lines would support the validity of the atmospheric analysis, confirm the abundance spread, and suggest that non-standard mixing in PMS stars is important.

Given this controversy, we have repeated Russell’s experiment, collecting our own data for several Pleiades G and K stars. We also obtained the data (including calibration frames) taken by Russell in 1993. These data were extracted, calibrated and analysed in exactly the same way as our own.

2. Observations and reduction

A sample of 6 late-G and early-K stars were selected from the catalogue of Soderblom et al. (1993a) on the basis of V (11.0 to 12.0) and $B - V$ (0.75 to 0.9) colours, and low $v \sin i$ ($< 10 \text{ km s}^{-1}$). These objects show a large spread in $A(\text{Li})$ ($= \log_{10} \left(\frac{N(\text{Li})}{N(\text{H})} \right) + 12$) at a given temperature, but have relatively low projected rotational velocities, simplifying the deblending and measurement of the lines. The objects have previously reported $A(\text{Li})$ values between 1.59 and 3.19 (Soderblom et al. 1993a). Two F stars were also observed for comparison, but their $v \sin i$ values were too large to attempt to determine abundances from the severely blended 6104 Å line (see below). The new spectroscopic data acquired for this study were taken on the 4.2 m William Herschel Telescope (WHT) on 1998 November 28 and 29, and 1999 December 22 and 23. The Utrecht Echelle Spectrograph (UES) was used for its high resolving power ($\sim 50\,000$), with the E31 (31 grooves mm^{-1}) grating. Typical exposure times of 6000–9000 s were used, split over several exposures in order to minimise cosmic-ray contamination. The central wavelength was chosen to give good coverage of both Li lines. Russell’s data were retrieved from the ING Data Archive (maintained by the Cambridge Astronomical Survey Unit). These data were obtained on 1993 January 8–10, using the same spectrograph and gratings, but a smaller EEV CCD and slightly shorter exposure times.

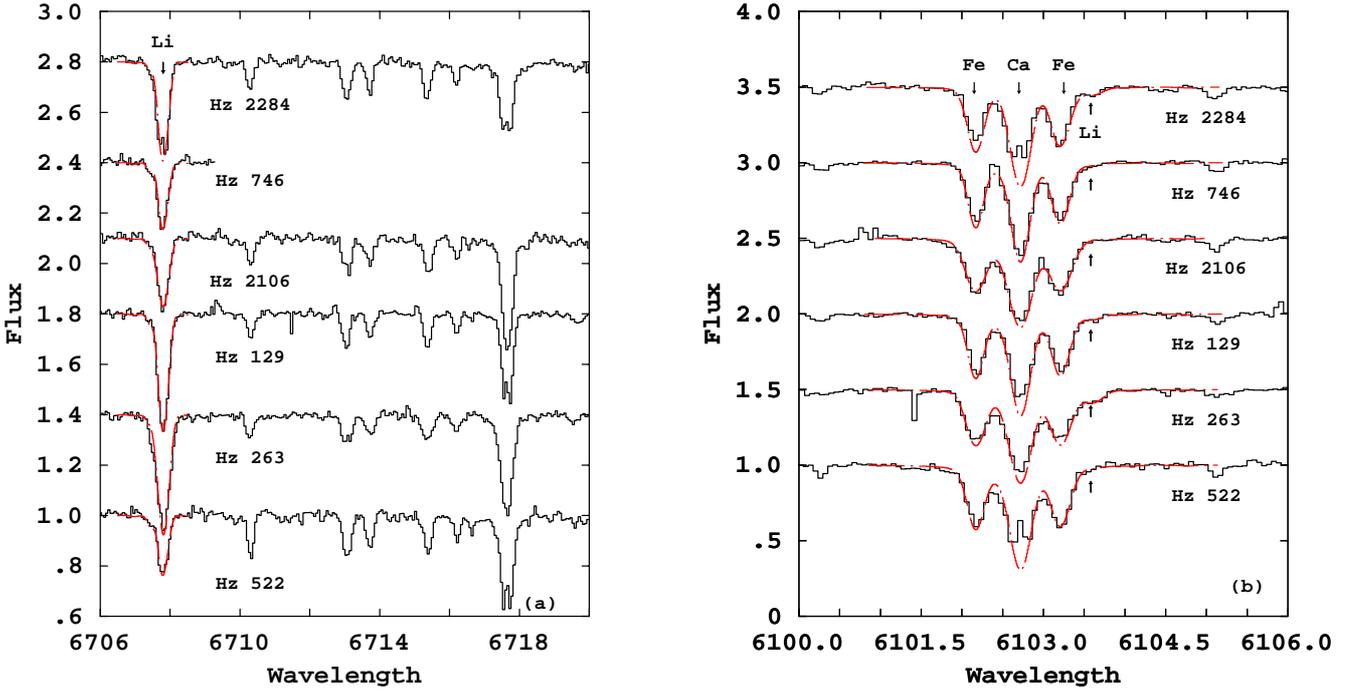


Fig. 1. Normalised spectra for our sample stars in the region of **a)** 6708 and **b)** 6104. Solid lines represent the observed data, while dashed lines represent the synthetic fits. In objects where the 6104 line was not detected, the syntheses are for $A(\text{Li}) = 0$.

Table 2. Object photometry (from Soderblom et al. 1993a), model parameters, S/N and resolution of spectra. Objects below the line are those in Russell’s sample.

| Object | $B - V$ | T_{eff} (K) | $v \sin i$ km s^{-1} | ξ km s^{-1} | S/N (6708) | S/N (6104) | $FWHM$ (6708) | $FWHM$ (6104) |
|----------|---------|-------------------------|----------------------------------|-----------------------------|-----------------|-----------------|--------------------|--------------------|
| Hz 1122 | 0.425 | 6535 | 28.6 ± 1.2 | 2.40 | 135 | 135 | 0.17 \AA | 0.16 \AA |
| Hz 233 | 0.493 | 6290 | 14.1 ± 0.7 | 1.80 | 140 | 115 | 0.17 \AA | 0.16 \AA |
| Hz 2284 | 0.743 | 5449 | 3.7 ± 0.8 | 2.88 | 90 | 95 | 0.17 \AA | 0.16 \AA |
| Hz 746 | 0.768 | 5383 | 4.8 ± 0.8 | 2.10 | 75 | 90 | 0.14 \AA | 0.12 \AA |
| Hz 2106 | 0.823 | 5245 | 8.0 ± 0.8 | 2.32 | 80 | 70 | 0.17 \AA | 0.16 \AA |
| Hz 129 | 0.830 | 5228 | 5.3 ± 1.4 | 2.02 | 95 | 110 | 0.14 \AA | 0.12 \AA |
| Hz 263 | 0.836 | 5213 | 7.8 ± 0.8 | 2.13 | 100 | 90 | 0.14 \AA | 0.12 \AA |
| Hz 522 | 0.879 | 5110 | 4.4 ± 0.8 | 2.34 | 80 | 80 | 0.17 \AA | 0.16 \AA |
| Hz 2311 | 0.780 | 5352 | 6.5 ± 0.8 | 2.3 | 40 | 30 | 0.16 \AA | 0.13 \AA |
| Pels 143 | 0.853 | 5177 | 5.2 ± 1.2 | 2.3 | 50 | 45 | 0.16 \AA | 0.13 \AA |
| Pels 19 | 0.853 | 5172 | 4.8 ± 1.4 | 2.3 | 75 | 65 | 0.16 \AA | 0.13 \AA |
| Hz 1095 | 0.858 | 5160 | 3.6 ± 0.8 | 2.3 | 75 | 90 | 0.16 \AA | 0.13 \AA |
| Pels 44 | 0.855 | 5167 | 3.9 ± 3.1 | 2.3 | 65 | 50 | 0.16 \AA | 0.13 \AA |
| Hz 522 | 0.879 | 5110 | 4.4 ± 0.8 | 2.34 | 65 | 70 | 0.16 \AA | 0.13 \AA |

Observational parameters are summarised for all datasets in Table 1. Target information is summarised in Table 2.

The usual calibration frames were taken including tungsten flat fields, bias frames and thorium-argon arc spectra. We also obtained a solar spectrum. The data were extracted and wavelength calibrated using the Starlink ECHOMOP (Mills et al. 1997) and FIGARO (Shortridge et al. 1999) packages. Scattered-light subtraction was performed during the ECHOMOP reduction, using inter-order regions. Continuum placement was determined by fitting a polynomial to line-free regions of the spectrum around the Li lines, as determined by a spectrum synthesis at the appropriate temperature and metallicity. The rms of this fit was

used to determine a conservative signal-to-noise (S/N) estimate, such that $\frac{1}{\text{rms}} = S/N$ (values are presented in Table 2). The theoretical S/N values, based simply on the number of detected photons, should be $\sim 30\%$ larger: the discrepancy probably arises from weak or unidentified lines, residual cosmic ray features or flat-fielding errors. Russell claimed S/N values of 100–180 for his observations, but these values are significantly larger than either the conservative S/N estimates or the theoretical S/N levels that we determine.

Figure 1 shows reduced spectra in the regions of 6708 and 6104 for our data. Spectra for those objects observed by Russell are presented in Fig. 2.

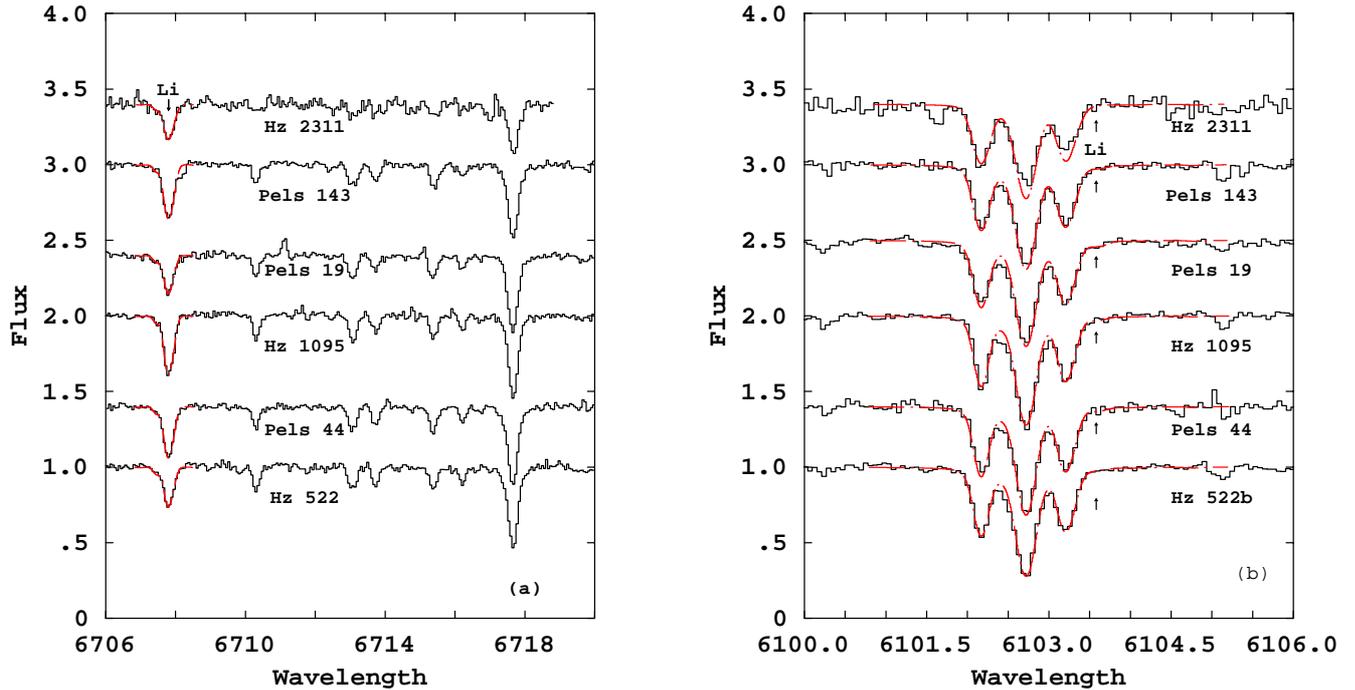


Fig. 2. Normalised spectra for Russell’s data in the regions of the a) 6708 and b) 6104 lines (solid line) and fitted synthetic LTE spectra (dashed line). Note that the spectra have been offset for clarity. Arrows indicate the wavelengths of the Li features.

3. Analysis

Effective temperatures were calculated from the $B - V$ photometry presented in Soderblom et al. (1993a) using the calibration of Böhm-Vitense (1981). The surface gravity was taken as 4.5 for all stars in the sample. The photometry, calculated T_{eff} , $v \sin i$ (taken from Queloz et al. 1998), microturbulent velocity (ξ – see below), S/N , and instrumental broadening ($FWHM$ – obtained from Gaussian fits to arc lines) values are presented in Table 2. The models used in the analysis were Kurucz, 1-D, homogeneous, LTE, ATLAS9 model atmospheres (Kurucz 1993) incorporating the mixing-length treatment of convection ($\alpha = 1.25$) without overshooting (Castelli et al. 1997). Before any analysis of the object spectra was undertaken, we used a high-resolution solar atlas (Kurucz et al. 1984), and solar spectra taken during our observing time, to tune the atomic parameters of the lines adjacent to Li. This was done by fitting a spectral synthesis to the data, assuming the solar parameters to be: $T_{\text{eff}} = 5777 \text{ K}$; $\log g = 4.44$; $\xi = 1.5 \text{ km s}^{-1}$; $v \sin i = 2 \text{ km s}^{-1}$; $A(\text{Fe}) = 7.54$; $A(\text{Ca}) = 6.36$. This assumed value for the microturbulence is a few tenths higher than frequently used for the Sun, but is the value espoused by Castelli et al. (1997) in their examination of the ATLAS9 model atmospheres. We will examine the effects of this assumption subsequently. The complete line lists used for the 6708 and 6104 regions are presented in Tables 4 and 5 (it should be noted that whilst all the lines listed were put into the syntheses, many had negligible equivalent width – hereafter EW). Damping constants were those provided by the Kurucz & Bell (1995) line list, except for the Ca I lines adjacent to 6104, and for the Li lines themselves, where the larger Anstree, Barklem O’Mara (ABO – Barklem et al. 2000) Van der Waals broadening

parameters were used. We also arbitrarily increased the damping constants for the strong Fe I lines (for which no ABO results are yet available) and as a result, drastically improved the fits to the line wings in the high resolution solar atlas (see Fig. 3). The gf values were varied for each line in turn, until the minimum chi-squared value for each line was obtained. The resultant line list and synthesis was broadened to the instrumental resolution, then checked against our observed solar spectrum. It was then used throughout the rest of the analysis. We note that if we had assumed a smaller value for the solar microturbulence then we would have simply increased the damping widths by a little more to compensate.

gf values were also obtained for ~ 20 Fe I lines in the ranges 6000–6150 Å and 6700–6750 Å (listed in Table 3, again by fitting the observed solar spectrum). The EW s of the lines (obtained for each object by direct integration below the apparent continuum) were then used to determine the microturbulence parameter for each Pleiades target in our sample. The most likely ξ value is taken to be that where there is no correlation between EW and abundance for the lines in the sample (Magain 1986). The lines measured had EW s between 0.01 Å and 0.16 Å. We find ξ values (listed in Table 2) of 2–3 km s^{-1} for the Pleiades targets and estimate that the maximum likely error in ξ is $\pm 0.5 \text{ km s}^{-1}$. For Russell’s data we did not have the same range of Fe I lines available. For these targets we simply adopted a mean Pleiades value of 2.3 km s^{-1} . These microturbulence values are larger by about 1 km s^{-1} than assumed by Boesgaard & Friel (1990) or measured by King et al. (2000). We are not concerned by this. Some of the difference can be attributed to using a slightly higher solar microturbulence, although as King et al. used different atmospheric models we would not necessarily expect agreement. A consistency check

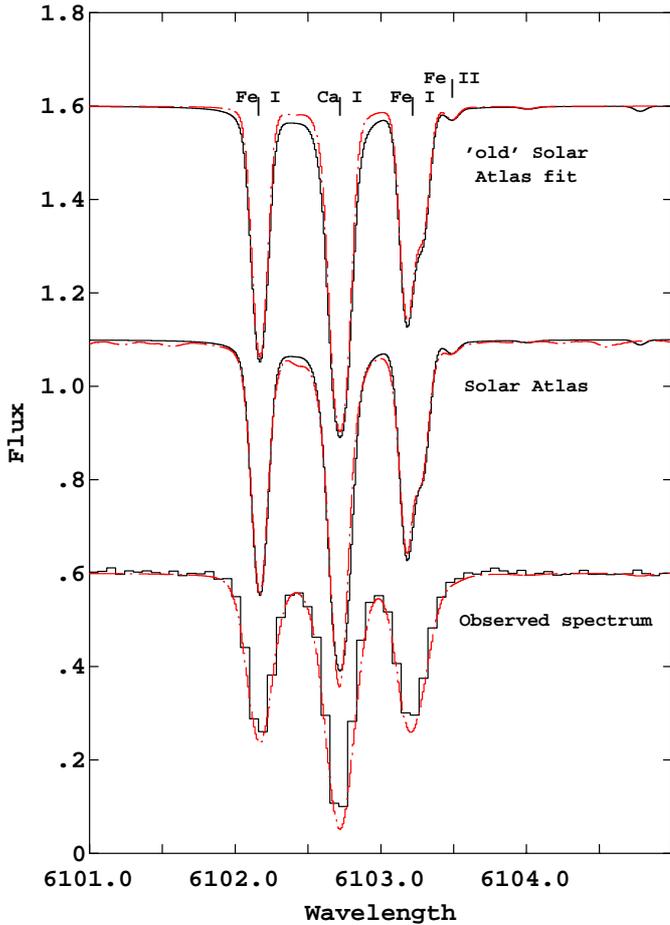


Fig. 3. Fits (dashed lines) to the solar atlas (top and middle) and observed solar spectrum (bottom) in the region of 6104, using gf factors determined for the lines. The top spectrum shows the synthesis using standard Van der Waals broadening co-efficients, while the ABO values were used for the other two syntheses (Sect. 3).

on the assumed values of T_{eff} and ξ is offered by our derived $[\text{Fe}/\text{H}]$ values. We find a mean of $[\text{Fe}/\text{H}] = -0.06 \pm 0.03$, in reasonable agreement with Boesgaard & Friel and King et al.

3.1. Fitting the lines

Once all the required model parameters were determined, lithium abundances were obtained by fitting a synthesized spectrum to the data using UCLSYN (Smith 1992; Smalley et al. 2001). In the case of 6708 the synthesized region was from 6706.5 Å to 6709.5 Å. The only significant line (apart from Li I) was the (partially-resolved) Fe I 6707.43 Å line. The 6708 Å line was treated as a quadruplet (see Table 4). The 6104 region was modelled between 6100.5 Å and 6105.5 Å. Here, the nearby Ca I, Fe I and Fe II lines were all important and the 6104 Å line was synthesized as a triplet (see Table 5). Abundances of Fe and Ca were fixed at $\text{solar} - 0.03$, or $A(\text{Fe}) = 7.51$ and $A(\text{Ca}) = 6.33$ (assuming a solar $[\text{Ca}/\text{Fe}]$ ratio). This iron abundance was determined spectroscopically by Boesgaard & Friel (1990). We use this value rather than our own derived value for each star, because we believe that some of these stars are considerably affected by large surface

Table 3. Wavelengths and gf factors for Fe I lines used in microturbulence determination (\ddagger and \dagger indicate lines which are blended)

| Wavelength (Å) | Calculated gf factor | gf factor | Excitation Potential |
|---------------------|------------------------|-------------|----------------------|
| 6024.049 | -0.250 | -0.120 | 4.549 |
| 6027.050 | -1.300 | -1.210 | 4.076 |
| 6055.992 | -0.550 | -0.460 | 4.733 |
| 6062.846 | -4.130 | -4.140 | 2.176 |
| 6065.805 | -4.168 | -4.168 | 3.301 |
| 6078.491 | -0.729 | -0.424 | 4.795 |
| 6078.999 | -1.200 | -1.120 | 4.652 |
| 6136.615 | -1.619 | -1.400 | 2.453 |
| 6136.993 | -3.202 | -2.950 | 2.198 |
| 6137.270 \ddagger | -2.252 | -1.944 | 4.580 |
| 6137.497 \ddagger | -2.601 | -3.263 | 3.332 |
| 6137.694 \ddagger | -1.788 | -1.403 | 2.588 |
| 6147.829 | -1.600 | -1.700 | 4.076 |
| 6705.101 | -1.248 | -1.433 | 4.607 |
| 6710.316 | -4.969 | -5.296 | 1.485 |
| 6713.046 \dagger | -1.653 | -1.889 | 4.607 |
| 6713.195 \dagger | -2.524 | -2.747 | 4.143 |
| 6725.353 | -2.300 | -2.506 | 4.103 |
| 6732.070 | -2.450 | -2.517 | 4.584 |
| 6733.151 | -1.600 | -1.758 | 4.638 |

Table 4. Line list for the region around 6708.

| Element | Wavelength (Å) | Excitation Potential (eV) | $\log gf$ |
|--------------|----------------|---------------------------|-----------|
| Fe 2 | 6706.880 | 5.956 | -9.840 |
| Si 1 | 6706.980 | 5.954 | -2.718 |
| Fe 1 | 6707.432 | 4.608 | -2.357 |
| Sm 2 | 6707.450 | 0.920 | -2.200 |
| V 1 | 6707.518 | 2.743 | -0.165 |
| Cr 1 | 6707.644 | 4.207 | -2.667 |
| Li 1 \star | 6707.754 | 0.000 | -0.431 |
| Li 1 \star | 6707.766 | 0.000 | -0.209 |
| Li 1 \star | 6707.904 | 0.000 | -0.773 |
| Li 1 \star | 6707.917 | 0.000 | -0.510 |
| Fe 1 | 6708.609 | 5.446 | -2.298 |
| Ti 1 | 6708.755 | 3.921 | 0.094 |
| Fe 2 | 6708.885 | 10.909 | 1.458 |

\star Indicates use of ABO/tuned values for the Van der Waals broadening coefficients – see Sect. 3.

inhomogeneities such as star spots – see Sect. 4.2. This might introduce errors into our $[\text{Fe}/\text{H}]$ values that would not have been present in the hotter F stars considered by Boesgaard & Friel. It might also of course introduce errors in our Li abundances, which we will subsequently consider at some length.

The lithium abundance was determined by varying it until a minimum value of chi-squared was obtained; 1- σ errors in abundance were found by searching for abundance values that increased this chi-squared value by 1. The EW for the Li lines were then determined from the synthetic spectra, though we stress the abundance is determined by the synthetic fit, not via a curve of growth. The results are given in Table 6.

The 6104 Å line is difficult to measure as it is very weak and lies in the red-ward wings of strong Ca I and Fe I lines, and next

Table 5. Line list for the region around 6104.

| Element | Wavelength (Å) | Excitation Potential (eV) | log <i>gf</i> |
|---------|-------------------|------------------------------|---------------|
| Co 1 | 6100.769 | 4.504 | -1.668 |
| Si 1 | 6102.136 | 5.984 | -2.120 |
| Fe 1 | 6102.159 | 4.608 | -2.692 |
| Fe 1 | 6102.173 | 4.835 | -0.454 |
| Si 1 | 6102.408 | 5.984 | -2.800 |
| Fe 1★ | 6102.606 | 4.584 | -2.501 |
| V 1 | 6102.706 | 3.245 | -0.751 |
| Ca 1★ | 6102.723 | 1.879 | -0.950 |
| Ti 1 | 6102.821 | 1.873 | -2.315 |
| Fe 1★ | 6103.186 | 4.835 | -0.721 |
| Fe 1★ | 6103.294 | 4.733 | -1.325 |
| Fe 2★ | 6103.496 | 6.217 | -2.224 |
| Li 1★ | 6103.538 | 1.848 | 0.101 |
| Li 1★ | 6103.649 | 1.848 | 0.361 |
| Li 1★ | 6103.664 | 1.848 | -0.599 |
| Si 1 | 6104.019 | 5.954 | -3.030 |
| Sm 2 | 6104.781 | 1.798 | 0.031 |

★ Indicates use of ABO/tuned values for the Van der Waals broadening coefficients – see Sect. 3.

to a weak Fe II feature, so high-resolution spectra are required to facilitate detection. In four cases 6104 can be clearly seen with a significant *EW* (Hz 2284, Hz 129, Hz 263 and Pels 19). In four cases the line is marginally detected. That is, there is a reduction in χ^2 when 6104 is added to the synthesis, but not at a level sufficient to claim a secure detection. For these objects (Hz 746, Pels 143, Hz 1095, Pels 44) we quote the best fit abundance, but caution the reader that the two-sigma errors in abundance are consistent with no Li at all. In cases where chi-squared was not improved by adding Li (Hz 522, Hz 2311 and Hz 2106), we instead estimated upper limits to the Li abundance by producing an increase in χ^2 consistent with a 99%-confidence interval.

4. Results

The Li abundances obtained from our syntheses are LTE values. The 6104 Å and 6708 Å lines are affected by small NLTE corrections which we apply using the code of Carlsson et al. (1994). Both LTE-derived and NLTE-corrected abundances are presented, together with synthetic *EWs*, in Table 6. LTE-derived and NLTE-corrected abundances are plotted in Fig. 4, with lines joining the LTE and NLTE abundances for each object. Note that the uncertainties quoted are statistical, relating to the fitting process, and do not include systematic errors, which we discuss below.

There is an apparent scatter in Li abundance from both lines, with a spread of ~ 0.7 dex for each line, although this could potentially be larger for 6104, due to the presence of upper limits. The abundances measured from the two lines do at least appear to be correlated. However, before we can accept this scatter as real, we need to consider possible sources of error in the synthetic abundance determinations.

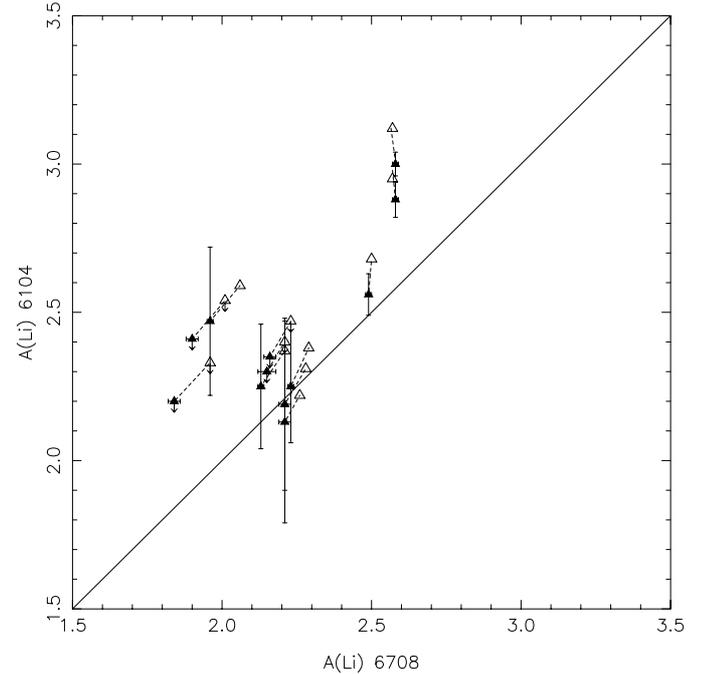


Fig. 4. LTE-derived (filled triangles) and NLTE-corrected (open triangles) $A(\text{Li})_{6104}$ versus $A(\text{Li})_{6708}$ for sample stars. Points for each object are connected by dotted lines.

4.1. Atomic parameter uncertainties

When fitting the Li lines, the main sources of error (aside from the statistical errors) which are likely to arise from the measurement process are the atomic parameters: damping and oscillator strengths.

Stark and Van der Waals damping effects arise from perturbations due to charged particles (Stark) and neutral hydrogen (Van der Waals) and shape the wings of the lines. Stark broadening is weaker than Van der Waals effects in the outer layers of the atmosphere, becoming important only deep within the star. Total removal of the Stark broadening affects derived Li abundances by only ~ 0.001 dex, whilst neglect of Van der Waals effects in the Li lines can lead to abundance variations of 0.022 dex for 6708, or 0.001 dex for 6104. The broadening of lines near Li, especially around 6104, can also affect the derived abundances, since the wings of the strong Ca I and Fe I lines contribute to absorption at the Li wavelength. In our syntheses we have used the best available (ABO) Van der Waals co-efficients (Barklem et al. 2000) for the Li I, and Ca I lines and tuned these coefficients for the Fe I lines to get a good fit to the solar atlas. Using the older Kurucz & Bell (1995) coefficients would result in approximately 0.05–0.25 dex higher Li abundances from the 6104 Å line, where the smaller increase is appropriate for our targets with the largest Li abundance. The increase is mainly due to the broad wings of the very strong Ca I line being interpreted as extra absorption due to Li.

The other source of atomic uncertainties is the oscillator strengths. These are difficult to measure reliably from astrophysical spectra. However, since we are not interested in the Ca and Fe lines, other than to ensure we get the best fits to the Li features, we have fitted the *gf*s for these other elements

Table 6. Synthetic Li EWs, EW of the core of H α , LTE-derived Li abundances, and NLTE-corrected Li abundances for sample spectra.

| Object | T_{eff} | H α EW | EW_{6708} | $A(\text{Li})_{6708}$ | $A(\text{Li})_{6708}$ | EW_{6104} (mÅ) | $A(\text{Li})_{6104}$ | $A(\text{Li})_{6104}$ | $\Delta A(\text{Li})^*$ |
|-----------------|------------------|-----------------|-----------------|-----------------------|-----------------------|------------------|-----------------------|-----------------------|-------------------------|
| | | (Å) | (mÅ) | LTE | NLTE | (mÅ) | LTE | NLTE | |
| H α 2284 | 5449 | 0.66 ± 0.02 | 138.9 ± 2.1 | 2.58 ± 0.01 | 2.57 | 13.6 ± 1.6 | 2.88 ± 0.06 | 2.98 | +0.41 |
| H α 746 | 5383 | 0.60 ± 0.02 | 86.2 ± 2.2 | 2.21 ± 0.02 | 2.25 | 2.8 ± 1.7 | 2.13 ± 0.34 | 2.22 | -0.03 |
| H α 2106 | 5245 | 0.47 ± 0.02 | 103.9 ± 2.5 | 2.16 ± 0.02 | 2.23 | ≤ 5.8 | ≤ 2.35 | ≤ 2.47 | ≤ 0.24 |
| H α 129 | 5228 | 0.46 ± 0.02 | 164.5 ± 0.9 | 2.49 ± 0.01 | 2.50 | 8.2 ± 1.5 | 2.56 ± 0.07 | 2.68 | +0.18 |
| H α 263 | 5213 | 0.40 ± 0.02 | 185.9 ± 1.9 | 2.58 ± 0.01 | 2.57 | 25.0 ± 2.5 | 3.00 ± 0.04 | 3.12 | +0.55 |
| H α 522 | 5110 | 0.61 ± 0.02 | 78.5 ± 2.1 | 1.84 ± 0.02 | 1.96 | ≤ 5.0 | ≤ 2.20 | ≤ 2.33 | ≤ 0.37 |
| H α 2311 | 5352 | 0.65 ± 0.04 | 83.5 ± 3.6 | 2.15 ± 0.03 | 2.21 | ≤ 4.3 | ≤ 2.30 | ≤ 2.40 | ≤ 0.19 |
| Pels 143 | 5177 | 0.66 ± 0.03 | 126.0 ± 2.7 | 2.21 ± 0.02 | 2.28 | 4.4 ± 2.3 | 2.19 ± 0.29 | 2.31 | +0.03 |
| Pels 19 | 5172 | 0.59 ± 0.02 | 84.7 ± 1.5 | 1.96 ± 0.01 | 2.06 | 8.4 ± 4.1 | 2.47 ± 0.25 | 2.59 | +0.53 |
| H α 1095 | 5160 | 0.61 ± 0.02 | 131.6 ± 1.8 | 2.23 ± 0.01 | 2.29 | 5.2 ± 2.1 | 2.25 ± 0.19 | 2.38 | +0.09 |
| Pels 44 | 5167 | 0.66 ± 0.02 | 113.6 ± 1.7 | 2.13 ± 0.01 | 2.21 | 5.2 ± 2.0 | 2.25 ± 0.21 | 2.38 | +0.17 |
| H α 522 | 5110 | 0.65 ± 0.02 | 86.7 ± 2.3 | 1.90 ± 0.02 | 2.01 | ≤ 8.1 | ≤ 2.41 | ≤ 2.54 | ≤ 0.53 |

* This is $A(\text{Li})_{6104} - A(\text{Li})_{6708}$ for NLTE abundances.

using a solar atlas and observed spectra (see Sect. 3). We did not fit the gf s for either of the Li lines, since the Li abundance in the Sun is low enough that the lines are barely visible, even in the high-resolution solar atlas. The values we have used for Li are those given in the Vienna Atomic Line Database (VALD – Piskunov et al. 1995) which is the best source for such data at the present time. The Li gf values given in VALD are also the same as those presented by Lindgard & Nielsen (1977). It is possible that the 6104 gf factors could have been wrongly estimated, which would affect the abundances derived from the line: uncertainties in the gf values are quoted at $<3\%$ for 6708 and $<10\%$ for 6104 (corresponding to abundance uncertainties of about 0.01 and 0.04 dex respectively) by Weiss (1963). We also determined a gf factor for the Fe II line adjacent to 6104, with the new value being 0.053 dex smaller than the value quoted in the original line list. The change in gf has a negligible impact on the 6104-derived Li abundances, although the inclusion of the Fe II line in the synthesis, is significant (see below).

4.2. Atmospheric uncertainties

Other than those uncertainties due to fitting the lines, there are likely to be systematic uncertainties in the determined abundances due to the atmospheric model parameters used. These might change the comparison of abundances derived from 6104 and 6708 or indeed inject scatter into the derived abundances from both lines. To gain an understanding of the effects that changes of T_{eff} , $\log g$, ξ and the metallicity of the atmosphere, we attempted to fit our spectra after perturbing each of these parameters in turn. The new Li abundances were then compared with the original fits to see what size abundance errors could result from plausible changes in the atmospheric parameters. Note that this procedure is more complex than simply re-generating curves of growth for each atmospheric model (which is often done in the literature). We find that, especially in the case of 6104, the deduced Li abundances vary by more

than would be expected from a simple curve of growth, because of the interplay with the wings of the strong adjacent lines and the presence of the nearby Fe II line.

Example results from these tests are listed in Table 7, for two stars (H α 263 and Pels 44) which are representative of the highest and lowest Li abundances found in our dataset. Of the atmospheric parameters, changes in T_{eff} have the most significant effect on abundance. The photometry errors were small, ~ 0.02 (Soderblom et al. 1993a), propagating to a temperature difference of about 50 K at 5300 K. A change in model temperature will affect abundances from both lines to almost the same extent and systematically in the same direction – about 0.12 dex per 100 K change in T_{eff} . The change in the 6104-derived abundance is about twice what one would expect from a simple consideration of the 6104 curve of growth, but appears more or less independent of the strength of the Li feature. The effects of changing ξ , $\log g$ and [Fe/H] by plausible amounts are much smaller, except in the case of very weak 6104-derived abundances. Here we find that the blending wings of the strong adjacent lines *are* sensitive enough to these parameters that they lead to additional Li abundance errors. It is worth noting here that assuming systematically lower ξ values for the Sun and Pleiades stars would make no systematic difference to the 6104-derived abundances, because we would simply have increased the damping widths of the nearby lines to compensate and match the solar spectrum. There would be a very small systematic increase in the 6708-derived abundances, but by no more than indicated in Table 7 for a small ξ change.

We can conclude from these considerations that plausible uncertainties in the atmospheric parameters *cannot* explain the observed ≥ 0.7 dex scatter in the abundances measured from both lines.

A further source of error is likely to be the assumption of a single-temperature, plane-parallel, homogeneous atmosphere. This is discussed at some length in Sect. 5. Here we note that the fits to some (but not all) of the Pleiades stars appear rather poor in the cores of the Fe and Ca lines around 6104 Å.

Table 7. Effects of different parameters on $A(\text{Li})$. Results are given for Hz 263 and Pels 44, assuming the baseline atmospheric parameters listed in Table 2. The first row gives the unperturbed LTE abundances. Subsequent lines give the abundance for the stated parameter variation relative to the initial model. We do not expect the abundances to be accurate to 3 decimal places, but these are included to illustrate the small scale of some of the variations.

| Parameter | Varies by | Hz 263 | | Pels 44 | |
|------------------|-------------------------|--------|--------|---------|--------|
| | | 6708 Å | 6104 Å | 6708 Å | 6104 Å |
| – | – | 2.584 | 3.000 | 2.128 | 2.250 |
| T_{eff} | –100 K | –0.125 | –0.125 | –0.121 | –0.125 |
| T_{eff} | +100 K | +0.121 | +0.094 | +0.117 | +0.125 |
| $\log g$ | +0.3 | –0.004 | 0.000 | –0.002 | –0.141 |
| [Fe/H] | +0.1 | +0.008 | 0.000 | –0.003 | +0.062 |
| ξ | +0.5 km s ^{–1} | –0.024 | –0.008 | –0.003 | –0.062 |

Table 8. T_{eff} values and NLTE-derived Li abundances from (Cols. 2–4) this paper and (Cols. 5–7) Russell’s published results.

| Object | T_{eff} (K) | This paper | | Russell(1996) | | |
|----------|----------------------|-------------|----------------|----------------------|-----------|----------------|
| | | EW (mÅ) | $A(\text{Li})$ | T_{eff} (K) | EW (mÅ) | $A(\text{Li})$ |
| 6708 | | | | | | |
| Hz 2311 | 5352 | 83.5 ± 3.6 | 2.21 ± 0.03 | 5240 | 141 ± 5.6 | 2.37 |
| Pels 143 | 5177 | 126.0 ± 2.7 | 2.28 ± 0.02 | 5020 | 139 ± 4.2 | 2.09 |
| Pels 19 | 5172 | 84.7 ± 1.5 | 2.06 ± 0.01 | 5020 | 95 ± 2.8 | 1.85 |
| Hz 1095 | 5160 | 131.6 ± 1.8 | 2.29 ± 0.01 | 5000 | 139 ± 3.8 | 2.08 |
| Pels 44 | 5167 | 113.6 ± 1.7 | 2.21 ± 0.01 | 4990 | 123 ± 3.8 | 2.01 |
| Hz 522 | 5110 | 86.8 ± 2.3 | 2.01 ± 0.02 | 4940 | 100 ± 4.3 | 1.79 |
| 6104 | | | | | | |
| Hz 2311 | 5352 | ≤4.3 | ≤2.40 | 5240 | 7.7 | 2.53 |
| Pels 143 | 5177 | 4.4 ± 2.3 | 2.31 ± 0.29 | 5020 | 7.2 | 2.37 |
| Pels 19 | 5172 | 8.4 ± 4.1 | 2.59 ± 0.25 | 5020 | 6.2 | 2.31 |
| Hz 1095 | 5160 | 5.2 ± 2.1 | 2.38 ± 0.19 | 5000 | 10.2 | 2.50 |
| Pels 44 | 5167 | 5.2 ± 2.0 | 2.38 ± 0.21 | 4990 | 11.2 | 2.55 |
| Hz 522 | 5110 | ≤8.1 | ≤2.41 | 4940 | 11.0 | 2.50 |

However, the wings of the lines seem to be well fitted, and rather than arbitrarily change the Ca and Fe abundances by considerably more than 0.1 dex (for which there is no physical motivation), we leave the abundances at the mean Pleiades value. The lack of a good fit in the cores of some of these lines is clear evidence that, at least for some stars, something is lacking in our atmospheric models. This is also clearly seen in some of the Ca 6718 Å lines in Fig. 1 in the form of central reversals or asymmetries. As this line is often used for doppler imaging of star spots on cool stars we take these anomalous spectral features to indicate the presence of large spotted regions on at least some of our stars.

4.3. Comparison with Russell’s results

The observations of Russell’s data were taken under similar conditions to our own, except that he used an EEV CCD which has a smaller pixel size than the SITE 1, and a different central wavelength. Russell’s analysis differs from our own in a number of ways. The most straightforward is in the temperature calibrations used. He makes use of the calibration of Bessell (1979):

$$T_{\text{eff}} = 8899 - 6103(B - V)_o + 1808(B - V)_o^2 \quad (1)$$

which was also used by Soderblom et al. (1993a). Our temperature calibration is that of Böhm-Vitense (1981). This

matches that used by Russell at 6000 K, however for the cooler stars considered here our temperatures are higher by ~150 K. Following our consideration of abundance errors from T_{eff} uncertainties (Sect. 4.2) we see that this difference should result in Russell obtaining smaller 6708-derived abundances (by ~0.18 dex) for a given EW . The 6104-derived abundance will also be smaller by a similar amount. Table 8 contains the abundances obtained both in this paper and by Russell, and the temperatures used in each analysis.

Our NLTE-derived 6708 abundances are systematically higher than those reported by Russell, by an average of 0.2 dex (using our temperatures), which suggests that the majority of the difference in these abundances is due to the different temperature calibrations used. There are also different measurement techniques to be considered. Russell simply fitted a Gaussian to 6708 and we can confirm Russell’s EW s when we model these spectra in the same way. However, our synthetic EW s are systematically *smaller* than reported by Russell, by an average of 10.7 mÅ. This appears to be mainly because the feature is not Gaussian. In particular, the Fe I line, blue-ward of the Li line is *not* adequately deblended in the Gaussian fit. Allowing for this discrepancy in EW , our abundances are still about 0.07 dex higher than Russell’s, which we attribute to his use of an older version of Kurucz’s Atlas atmospheres. An exception to this is Hz 2311 (which was not included when calculating the mean abundance and EW differences mentioned

above), where our abundance is lower than that determined by Russell, and our EW value for the star is much lower than Russell reported. Why this should be the case is unclear, although this object has the lowest S/N of any in our sample, so there could be some major differences in continuum placement between the two objects.

6104 abundances determined using our temperatures are *smaller* by 0.1 to 0.3 dex, and our synthetic 6104 EW s seem to be smaller by 2–6 mÅ than those deduced by Russell. The abundance discrepancy would be about 0.18 dex wider if we had used Russell’s temperature scale. The exception is Pels 19, where our EW (and abundance) are both larger than previously reported. Russell did not publish his reduced spectrum for this object, so it is difficult to ascertain where such a discrepancy could have arisen. 6104 is present in the spectrum of Pels 19 (see Fig. 2), where no line is clearly visible in Pels 143 (even though Russell reports a larger EW for Pels 143). We have also obtained only upper limits to the abundance for Hz 2311 and Hz 522, where Russell claimed to have detected 6104.

We believe that these important differences, upon which our conclusions (and those of Russell) hinge, can be traced to the comprehensiveness of the fitting and synthesis techniques employed. In the case of 6104, Russell used two different techniques, both of which are open to criticism: fitting all the (strong Fe I and Ca I in addition to Li I 6104) lines around 6104 simultaneously with Gaussians; and fitting Gaussians to the (strong) Fe and Ca lines near Li 6104 (but omitting the weak Fe II line), subtracting the synthesis from the spectrum and then fitting the residual with another Gaussian. We believe this neglect of Fe II, along with the non-Gaussian nature of the surrounding strong, damped lines, could easily result in over-estimates of the 6104 EW and Li abundance. As 6104 is also a triplet, it is unlikely to be well represented by a Gaussian, and the red-most Fe I feature is actually a blend of two lines (this can just be seen in the solar atlas of this region – Fig. 3).

We gauged the magnitude of these problems by running the synthesis for a line list containing (a) the Fe I, Ca I and Fe II lines and (b) the Fe I and Ca I lines only, in addition to the Li triplet. The Li abundances obtained in the absence of the Fe II line appear to show a trend: the abundance is *over-estimated* by an amount which increases for the objects with smaller Li abundance (from the 6708 line). We would obtain Li abundances that are higher by between 0.02 and 0.10 dex as a result of neglecting the Fe II line, which would turn our upper limits into marginal detections. Omitting other weak lines from the list (while including Fe II) has a negligible effect on the abundance and EW attributable to 6104. The neglect of the damping wings on the Li abundance can be judged from our change from the Kurucz & Bell (1995) Van-der-Waals coefficients to the larger values required to fit the solar atlas. The lines are more closely approximated by Gaussians in the former case and as mentioned in the last section, result in Li abundances about 0.05–0.25 dex higher than when the broader line wings are used. Again, the biggest effect is for the objects with the weakest Li. We conclude that both the neglect of the Fe II line and the (implicit) neglect of the broad damping wings by assuming Gaussian line profiles conspire to produce larger 6104-determined Li abundances, such that the lowest Li

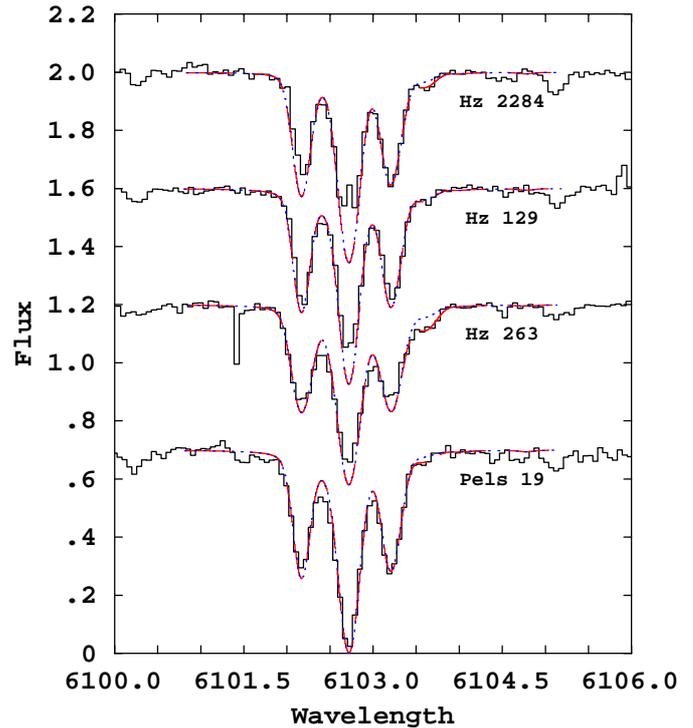


Fig. 5. Spectra of objects with firm 6104 detections (solid lines) in the region of the 6104 Å Li I line, showing LTE syntheses for abundances determined from 6104 (dashed) and 6708 (dotted) lines.

abundances would be increased the most. This would raise the average Li abundance and reduce the apparent abundance scatter deduced from this line. It might also lead to claims of detection for 6104, where in reality the line was too weak to be seen. It is worth noting however, that Russell’s conclusion that the spread in 6708-derived Li abundances was larger than that from 6104 can also be explained, in part, by the much larger 6708-derived Li abundance found for Hz 2311 by Russell.

4.4. 6104 versus 6708

In addition to scatter in Li abundances from both 6708 and 6104, we find that some 6104-derived NLTE-corrected abundances are higher than the corresponding 6708 values. The four objects where this is clearly the case are: Hz 2284 ($A(\text{Li})_{6104-6708} = 0.41 \pm 0.06$ dex), Hz 129 (0.18 ± 0.07 dex), Hz 263 (0.55 ± 0.04 dex) and Pels 19 (0.53 ± 0.25 dex). These stars are in fact the only ones where the 6104 Å line is clearly detected. To emphasize these discrepancies, in Fig. 5 we show LTE syntheses for the 6104 region using the LTE Li abundance suggested from the 6708 line and the LTE Li abundance fitted to the observed 6104 region. Temperature errors are probably not the culprit here because a 100 K temperature increase causes $A(\text{Li})_{6104}$ to increase by around 0.12 dex, but affects the 6708-derived abundances in a similar way. As discussed in Sects. 4.1 and 4.2, the differential abundance errors due to uncertainties in ξ , $\log g$ and the gf values are probably quite small in these stars, though not negligible. This abundance discrepancy *might* be present in the other stars, once the large errors in the 6104-derived abundance are taken into account, but

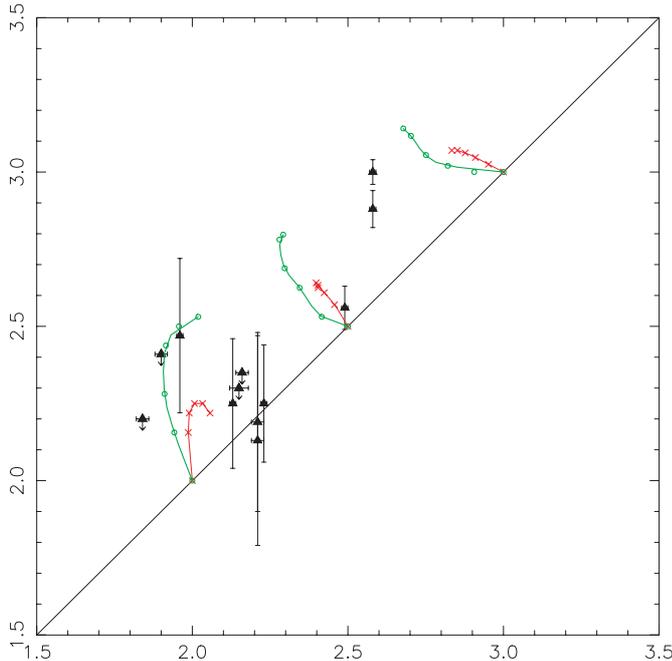


Fig. 6. LTE $A(\text{Li})_{6104}$ versus $A(\text{Li})_{6708}$ for sample stars. The curves represent the effect star spots would have on the abundances for a star with $T_{\text{eff}} = 5250$ K. Crosses represent the case where the spotted area is 1000 K cooler than the stellar surface, while circles show regions where the temperature difference is 1500 K. The symbols mark spotted areas of 0%, 10%, 20%, 30%, 40% and 50%. See also Sect. 5.

equally, the data are also consistent with good agreement between abundances determined from 6104 and 6708 for these stars.

The difference between the 6708 and 6104 abundances has been exacerbated by the application of NLTE corrections, as can be seen in Fig. 6. At the effective temperatures of our targets, and for low Li abundances, the NLTE corrections affect both lines roughly equally, increasing the determined abundances by 0.1 dex. At larger abundances, the NLTE corrections to the 6708 abundance become small and then reverse sign, whereas the 0.1 dex correction to the 6104 abundance remains roughly constant (see Carlsson et al. 1994).

We conclude, on the basis of the models that are available to us, that there is broad agreement and at least a correlation between the 6104 and 6708 abundances. However for some, but not necessarily all, of the stars we have investigated, the 6104-determined Li abundance gives higher values (by 0.2–0.5 dex) than that from 6708.

5. Discussion

The main aim of this study was to investigate whether the Li abundances determined from the subordinate line at 6104 Å agreed with those derived from the 6708 Å resonance line. Such an agreement would lend confidence to the atmospheric approximations and NLTE corrections used in Li studies, and might imply that the spread in abundance previously reported from the 6708 line alone was indicative of a physical

mechanism which could produce star-to-star differences in Li abundance during the approach to the ZAMS.

In our analysis, we find a scatter of ~ 0.7 dex from *both* 6708 and 6104 (although the 6104 spread could be larger still, due to upper-limit estimates for some of the objects). The scatter is not explained by the uncertainties considered for either line. We find a broad correlation between the abundances from the two lines although for some stars there is an indication that the 6104-determined abundance is still 0.2–0.5 dex higher. The reason our results do not entirely agree with those of Russell (1996), who found that the 6104-derived abundances were higher and showed less scatter than those from 6708, can be traced to: (a) The large 6708-derived abundance for Hz 2311 found by Russell, which we have not been able to confirm. This increases the scatter in Russell’s 6708-derived abundances; and (b) Russell’s neglect of the strong, non-Gaussian damping wings of lines that blend with 6104 and the neglect of a weak Fe II line, both of which might have been interpreted as Li absorption.

Although the abundance scatter derived from both lines supports the claim that the abundance spread is real, the disagreement in abundance for some cases does still illustrate a deficiency in our understanding of the stellar atmospheres. Due to their ease of computation, one-dimensional atmospheres have been used for most abundance determinations until recently. However, they do not allow for the existence of inhomogeneities such as star spots on stellar surfaces, which are certainly known to exist in young, magnetically active, late-type stars and particularly in the Pleiades G and K stars (e.g. Krishnamurthi et al. 1998). Doppler imaging study of the Pleiades G-type star ($T_{\text{eff}} = 5845$ K) Hz 314 (Rice & Strassmeier 2001) showed that the star had cool spots at or near the pole, and within the equatorial regions. The temperatures of the spots varied from 4400 K to 5400 K, with the average being ~ 4700 K. Spot areas have been measured spectroscopically for several highly-active G and K stars by O’Neal et al. (1998), who find spot coverage of 3–56%, and temperature differences between spotted and “quiet” (unspotted) regions ranging from 750 K to 1900 K.

The presence of spots could alter our conclusions in two ways: they might reduce the spread in Li abundances significantly in a group of stars with differing spot coverage (this has previously been explored by Soderblom et al. 1993a and Barrado y Navascúes et al. 2001, who conclude that the effect is not large enough). However, 6104 and 6708 might be affected differently due to their differing curve of growth temperature sensitivities, so differing spot coverage might well explain why some stars have agreement between 6708- and 6104-derived abundances while others reveal a higher abundance from 6104.

In order to probe what effect star spots might be expected to have on the abundances determined in this paper, we used a two-component, one-dimensional atmospheric simulation (TCODAS) technique included in the UCLSYN code.

In the TCODAS models we balanced the spot and unspotted (quiet) star temperatures and areas, so that the luminosity-weighted average T_{eff} would remain the same, using

$$aT_{\text{eff}}^4 = a_{\text{cool}}T_{\text{cool}}^4 + a_{\text{star}}T_{\text{star}}^4 \quad (2)$$

where a_{cool} and T_{cool} are the cool-region area and temperature, and a_{star} and T_{star} are the area and temperature for the rest of the star. The areas are normalised to unity, such that:

$$a_{\text{star}} + a_{\text{cool}} = 1 \quad (3)$$

$\Delta T (= T_{\text{star}} - T_{\text{cool}})$ and a_{cool} were fixed at a number of discrete points, then Eq. (2) was solved for the appropriate T_{eff} . We assume that the cool regions are uniformly distributed across the star to avoid difficulties in modelling line-profile asymmetries.

The relative-light (LR) contributions from the two components were flux weighted using

$$LR_{\text{cool}} = \frac{a_{\text{cool}} \times T_{\text{cool}}^4}{T_{\text{eff}}^4} \quad (4)$$

and

$$LR_{\text{star}} = \frac{a_{\text{star}} \times T_{\text{star}}^4}{T_{\text{eff}}^4} \quad (5)$$

We generated synthetic (LTE) spectra (at 6104 and 6708) using two component models with a luminosity-weighted average T_{eff} of 5250 K, spot coverage of between 10 and 50 percent of the visible hemisphere and a temperature difference of either 1000 K or 1500 K between spotted and unspotted components. Finally we fitted our two-component syntheses with one component models at both 6104 and 6708. The resulting abundances are plotted in Fig. 6. These suggest that the abundances for Hz 263, Hz 2284 and Pels 19 (and Hz 129) could potentially be explained by the presence of star spots on these objects with coverage fractions of 10–50 percent and ΔT of 1000–1500 K. Note that the results obtained from TCODAS are LTE abundances, since we do not have access to NLTE syntheses, and application of 1-D NLTE corrections to the results would most likely not be valid.

Is there any evidence to support the notion that those stars with significant discrepancies between their 6708- and 6104-derived abundances are the most magnetically active and spotted? We have no direct information on this and we must recognize that spot coverage might change with time, so unless observations of magnetic-activity indicators are co-temporal, they should be treated cautiously. There are indications of spot activity in the line profiles of Hz 263, Hz 2284 and Hz 129 (see Figs. 1, 2 and 5). Several line cores are filled in, especially the Ca I lines at 6102 Å and 6718 Å. It is just such signatures which are used to make doppler maps of star-spot distributions on more rapidly-rotating stars. However, we see little evidence of this in Pels 19, and similar signs of spot activity are present in Hz 2311 and Hz 522 (our observation rather than Russell’s), where the 6708- and 6104-derived Li abundances *might* be consistent (although the constraints are not strong and discrepancies of 0.2–0.3 dex cannot be ruled out).

A more quantitative magnetic-activity indicator could be the X-ray luminosity. Unfortunately, measurements are not available for all our stars and X-ray luminosity could easily vary by factors of 2–3 over time. A better diagnostic is the strength of H α measured from the same spectra as the Li abundances. Soderblom et al. (1993b) have investigated H α emission in the Pleiades. They found that late-G and early-K stars

exhibit H α absorption with a chromospherically-filled core. The amount of filling correlates with the rotation rate and other activity indicators. The strength of the underlying photospheric absorption is a function of T_{eff} . If, however, we make the reasonable assumption that this intrinsic absorption is uniform across the narrow T_{eff} range considered here, then we can use the EW of the H α core (1 Å either side of the line centre) to rank our targets in order of magnetic activity. These H α core EW s are listed in Table 6. All of the targets exhibit H α absorption, so it is the stars with the smallest EW s that are the most active – namely, Hz 263, Hz 129 and Hz 2106. Two of these have discrepant 6708- and 6104-derived abundances, whilst the third might not have. However, Hz 2284 is ranked as one of the least active stars by this method, yet it does show an abundance discrepancy from the two lines, along with signs of spot activity in its Ca I line profiles.

In summary the supporting evidence for a direct relationship between star spots and a discrepancy in Li abundance measured from the resonance and subordinate lines is ambiguous at present. The most active stars do seem to exhibit a discrepancy but there are counter examples as well. It should be made clear that the “spot” areas and temperature differences are not rigorously determined, and so should be treated only as fitting factors for use with the models, and not as actual areas or temperatures. We also remind the reader that changes in EW (and therefore changes in derived abundance) due to spot coverage (and spot coverage itself) vary over time. Jeffries et al. (1994) showed that 6708 was modulated by star spots during a rotation cycle in BD+22 4409, a young, active star. The line strength was observed to vary by $10 \pm 3\%$ (equivalent to an abundance variation of ~ 0.15 dex within a one-component model) over the 10-hour rotation period. Over longer time-scales, Jeffries (1999) reported no variability larger than 0.1 dex on one-year timescales in a group of Pleiades K stars, but considered that there might be variations of 0.2–0.3 dex over 10 years. Finally, we note that there are differences in the two observations of Hz 522 used in this work: the lines in the spectra obtained by Russell are stronger. This is consistent with an increase in spot coverage between the two sets of observations, resulting in an *apparent* abundance decrease of 0.06 ± 0.02 dex between 1993 and 1998, assuming a one-component atmospheric model. If this were typical of the magnitude of this effect, it is clear that only a small fraction of the Li abundance spread could be accounted for in this way. Star spots could however, account for the majority of the discrepancies between abundances derived from 6104 and 6708 which arise due to the use of single-component models.

The fact that we can obtain agreement between the 6708- and 6104-derived abundances with relatively minor and plausible changes to the atmospheric structure (namely the introduction of star spots) without altering the size of the scatter observed in both the 6708 and 6104 abundances might support the idea that this abundance scatter is real. However, it is still possible that this agreement is coincidental and major revisions to our understanding of these young stellar atmospheres will be required. A cautionary note should be that scatter has also been observed in the potassium abundances of Pleiades stars from the K I 7699 Å line, which is formed under similar conditions

to 6708 (Soderblom et al. 1993; Stuik et al. 1997; Jeffries 1999; King et al. 2000). As there are no plausible physical mechanisms to produce potassium depletion in these objects, this result still points to a deficiency in the atmospheric modelling. King et al. point to chromospheric activity altering the ionisation balance in the line formation region as being culpable. 6104 is formed a little deeper in the atmosphere than 6708, although there is plenty of overlap. It is beyond the scope of this paper to investigate whether plausible changes in the ionisation balance might also be able bring the 6104- and 6708-determined abundances into agreement, whilst at the same time significantly reducing the apparent scatter in Li and/or K abundances, though such an investigation is now called for.

6. Summary

We have obtained high resolution spectroscopy of a sample of 11 Pleiades late-G and early-K stars, covering a relatively narrow range of effective temperatures, of which six were observed by Russell (1996). These spectra were consistently reduced and analysed. One object, Hz 522, was included in both sets of observations.

- We measured the Li I 6708 Å resonance line in all the objects and determined Li abundances by fitting atmospheric syntheses. We obtained NLTE-Li abundances which were systematically higher than those reported by Russell, by an average of 0.2 dex. Most of this difference could be explained by the different temperature calibrations used in the two analyses. When the same temperatures reported by Russell were used, the difference between reported abundances for the lines was reduced to about 0.05 dex.
- We have also been able to measure Li abundances using the weak, subordinate Li I 6104 Å line in eight of our sample objects and have found upper limits for the remainder. The LTE abundances (or upper limits) derived from the 6708 Å and 6104 Å lines are reasonably well correlated, and agree within their errors, for most of our targets. However, for several objects the abundance derived from 6104 Å is significantly higher than from 6708 Å. NLTE corrections act to increase this discrepancy. For the sub-sample observed by Russell, we find that his multiple-Gaussian fitting technique has overestimated the strength of the 6104 line when compared with our spectral synthesis. This can be attributed to the the presence of a weak Fe II line close to the 6104 Å line, and the broad damping wings of the nearby Ca I and Fe I lines. Neglect of these leads to Li abundance overestimates of 0.05–0.35 dex, such that the overestimates are larger for those objects with weaker Li lines. It can also lead to the detection of an Li feature where none is present. This could account for the reduced scatter in Li abundances from the 6104 Å line (compared with the 6708 Å line) reported by Russell.
- A Li abundance scatter was observed from both lines: of order ~0.7 dex for 6708, and at least 0.7 dex for 6104, although this could conceivably be larger due to the presence of upper limits. We found no evidence of a reduced scatter in the abundances determined from 6104, contrary to

the conclusions of Russell (see above). The implications of this spread are either that there is real star-to-star scatter present, or that the agreement between the lines is coincidental and some (or all) of the spread is due to problems with the atmospheric models.

- Some of our spectra show signs of atmospheric inhomogeneities (star spots), namely filling or reversals in Ca and Fe lines. We considered the effects of star spots on the Li abundances, by using a two-component synthesis, and found that the presence of such spots could explain the Li abundance discrepancy found between the resonance and subordinate lines. Differences in their depth of formation and excitation potentials mean they react differently to changes in temperature. Although there is some evidence that the most magnetically active stars in our sample are indeed those that show significant discrepancies in their Li abundances as estimated from the two lines; counter examples are also seen. Therefore, introduction of cooler regions on to the star should only be regarded as a plausible explanation for our observations at this stage. Whilst star spots might be able to bring abundances from the two lines into agreement, they cannot significantly reduce the apparent spread in Li abundances among these cool Pleiades objects.

Acknowledgements. The William Herschel and Isaac Newton Telescopes are operated on the island of La Palma by the Isaac Newton Group in the Spanish Observatorio del Roque de los Muchachos of the Instituto de Astrofísica de Canarias. The authors acknowledge the travel and subsistence support of the UK Particle Physics and Astronomy Research Council (PPARC). AF was funded by a PPARC postgraduate studentship. Computational work was performed on the Keele, St. Andrews and Open University nodes of the PPARC funded Starlink network. This research has made extensive use of NASA's Astrophysics Data System Abstract Service.

References

- Barrado y Navascués, D., García López, R. J., Severino, G., & Gomez, M. T. 2001, *A&A*, 371, 652
- Barklem, P. S., Piskunov, N., & O'Mara, B. J. 2000, *A&AS*, 142, 467
- Boesgaard, A. M., & Friel, E. 1990, *ApJ*, 351, 480
- Böhm-Vitense, E. 1981, *ARA&A*, 19, 295
- Carlsson, M., Rutten, R. J., Bruls, J. H. M. J., & Shchukina, N. G. 1994, *A&A*, 288, 860
- Castelli, F., Gratton, R. G., & Kurucz, R. L. 1997, *A&A*, 318, 841
- Chaboyer, B., Demarque, P., & Pinsonneault, M. H. 1995, *ApJ*, 441, 876
- Duncan, D. K., & Jones, B. F. 1983, *ApJ*, 271, 663
- Giampapa, M. S. 1984, *ApJ*, 277, 235
- Gray, D. F. 1992, *The observation and analysis of stellar photospheres* (Cambridge University Press)
- Houdebaine, E. R., & Doyle, J. G. 1995, *A&A*, 302, 861
- Jeffries, R. D. 1999, *MNRAS*, 309, 189
- Jeffries, R. D. 2000, *Stellar Clusters and Associations: Convection, Rotation, and Dynamos*, ed. R. Pallavicini, G. Micela, & S. Sciortino (San Francisco), ASP Conf. Ser., 198, 245
- Jeffries, R. D., James, D. J., & Thurston, M. R. 1998, *MNRAS*, 300, 550
- Jeffries, R. D., Byrne, P. B., Doyle, J. G., et al. 1994, *MNRAS*, 270, 153

- Jones, B. F., Shetrone, M., Fischer, D., & Soderblom, D. R. 1996, *AJ*, 112, 186
- Jones, B. F., Fischer, D., Shetrone, M., & Soderblom, D. R. 1997, *AJ*, 114, 352
- King, J. R., Krishnamurthi, A., & Pinsonneault, C. P. 2000, *AJ*, 119, 859
- Krishnamurthi, A., Terndrup, D. M., Pinsonneault, M. H., et al. 1998, *ApJ*, 493, 914
- Kurucz, R. L. 1993, Kurucz CD-Rom, Atlas 9 (SAO, Cambridge)
- Kurucz, R. L., & Bell, B. 1995, Atomic Line Data, Kurucz CD-ROM No. 23 (Cambridge, Mass.: Smithsonian Astrophysical Observatory)
- Kurucz, R. L., Furenlid, I., Brault, J., & Testerman, L. 1984, Solar Flux Atlas from 296 to 1300 nm (National Solar Observatory, Sunspot, New Mexico)
- Lindgard, A., & Nielsen, S. E. 1977, Atomic Data and Nuclear Data Tables, 19, 533
- Magain, P. 1986, *A&A*, 163, 135
- Martín, E. L. 1997, *Mem. Soc. Astron. Ital.*, 68, 905
- Messina, D. 2001, *A&A*, 371, 1024
- Mills, D., Webb, J., & Clayton, M. 1997, Starlink User Note 152.4
- O'Neal, D., Neff, J. E., & Saar, S. H. 1998, *ApJ*, 507, 919
- Pasquini, L., Randich, S., & Pallavicini, R. 1997, *A&A*, 325, 535
- Piskunov, N. E., Kupka, F., Ryabchikova, T. A., Weiss, W. W., & Jeffery, C. S. 1995, *A&AS*, 112, 112
- Queloz, D., Allain, S., Mermilliod, J.-C., Bouvier, J., & Mayor, M. 1998, *A&A*, 335, 183
- Randich, S. 2001, *A&A*, 377, 512
- Randich, S., & Pallavicini, R. 1991, *Mem. Soc. Astron. Ital.*, 62, 75
- Russell, S. 1996, *ApJ*, 463, 593
- Rice, J. B., & Strassmeier, K. G. 2001, *A&A*, 377, 264
- Shorridge, K., Meyerdierks, H., Currie, M., et al. 1999, Starlink User Note 86.17
- Smalley, B., Smith, K. C., & Dworetzky, M. M. 2001, UCLSYN v3.1 User Guide, incorporating BINSYN and TELSYN
- Smith, K. C. 1992, Ph.D. Thesis, University of London
- Soderblom, D. R., Jones, B. F., Stauffer, J. R., & Chaboyer, B. 1995, *AJ*, 110, 729
- Soderblom, D. R., Jones, B. F., Balachandran, S., et al. 1993a, *AJ*, 106, 1059
- Soderblom, D. R., Stauffer, J. R., Hudon, J. D., & Jones, B. F. 1993b, *ApJS*, 85, 315
- Stuik, R., Bruls, J. H. M. J., & Rutten, R. J. 1997 *A&A*, 322, 911
- Thorburn, J. A., Hobbs, L. M., Deliyannis, C. P., & Pinsonneault, M. H. 1993, *ApJ*, 415, 150
- Weiss, A. W. 1963, *ApJ*, 138, 1262